

Correlating vapour uptake with the luminescence quenching of poly(dendrimer)s for the detection of nitro group-containing explosives

Kinitra L. Hutchinson^A, Beta Z. Poliquit^A, Andrew J. Clulow^A , Paul L. Burn^{A,*} , Ian R. Gentle^A and Paul E. Shaw^A

For full list of author affiliations and declarations see end of paper

***Correspondence to:**

Paul L. Burn
 Centre for Organic Photonics & Electronics, School of Chemistry and Molecular Biosciences, The University of Queensland, Qld 4072, Australia
 Email: p.burn2@uq.edu.au

Handling Editor:

Curt Wentrup

Received: 4 July 2023

Accepted: 8 August 2023

Published: 6 September 2023

Cite this:

Hutchinson KL *et al.* (2023)
Australian Journal of Chemistry
76(10), 677–685. doi:[10.1071/CH23131](https://doi.org/10.1071/CH23131)

© 2023 The Author(s) (or their employer(s)). Published by CSIRO Publishing.

This is an open access article distributed under the Creative Commons Attribution-NonCommercial-NoDerivatives 4.0 International License ([CC BY-NC-ND](https://creativecommons.org/licenses/by-nc-nd/4.0/))

OPEN ACCESS

ABSTRACT

Thin films of two poly(dendrimer)s were studied for the detection of trace quantities of nitro-based taggants and explosives. The poly(dendrimer) structures consist of side chain-conjugated triphenylamine-based dendritic chromophores attached to a non-conjugated polymer backbone. The poly(dendrimer)s differ in terms of the conjugation length, steric bulk and surface groups of the chromophores and we investigated the effects of these differences on sensing performance. We found that the addition of first-generation biphenyl-based dendrons to the chromophores of one of the polymers, **P2**, resulted in greater photoluminescence quenching, sensitivity and recovery to pulses of the vapours of the nitroaliphatic taggant 2,3-dimethyl-2,3-dinitrobutane (DMNB) and the nitroaromatic analyte 2,4-dinitrotoluene (2,4-DNT) compared with the other polymer, **P1**. We employed neutron reflectometry to characterise the vapour uptake of both poly(dendrimer)s and a structurally similar triphenylamine-based dendrimer **DI** for comparison. The results show that the **P2** has a mass density of 0.91 ± 0.01 v. 1.01 ± 0.01 g cm⁻³ for both **P1** and **DI** and can absorb at least twice the amount of 2,4-DNT. These results show how increasing the dendritic character of the poly(dendrimer) architecture provides a route for optimising vapour uptake and improving sensing performance in the solid state.

Keywords: dendrimers, explosive detection, luminescence, neutron reflectometry, photoinduced electron transfer, polymers, sensitivity, thin films.

Introduction

Fluorescent sensing materials provide a means of detecting nitro group-containing explosive vapours with high sensitivity by reversible oxidative quenching.^{1,2} That is, the materials are luminescent in the absence of the explosive, but in its presence, the exciton that is formed upon photoexcitation is oxidised by the explosive leading to non-radiative decay of the excited state and the luminescence being quenched. This approach is particularly attractive when the sensing material can be incorporated as a thin film into detectors that are low-power, mechanically robust and lightweight.³ Conventional chemical sensors based on analytical approaches such as mass spectroscopy are typically unsuitable for miniaturisation and detection of explosives in the field, so fluorescence-based sensors have the potential to meet the need for truly portable vapour sensors.⁴

The physical characteristics of the sensing material are critical to the detector performance and its sensitivity.^{5,6} The earliest work on the detection of nitro group-containing explosives and taggants utilised fluorescent polymers composed of a conjugated backbone, and such materials have been widely studied.⁷ The advantage of soluble conjugated polymers is that they can be easily processed into thin films, and the original work suggested that the polymeric systems had an amplified fluorescence quenching response that increased their sensitivity, improving their level of detection.⁸ Fluorescent dendrimers have also been shown to be capable of reversibly detecting nitro group-

containing explosives.⁹ However, one of the issues of fluorescence-based detection is selectivity towards the desired analyte, e.g., just the nitro group-containing explosives and taggants. In a key breakthrough, it was shown that fluorescent dendrimers can be selective to nitro group-containing explosives.¹⁰ The detection of explosive vapours involves two key processes: the diffusion of the analyte into the film and the photoinduced electron transfer (PET) that leads to the quenching of the luminescence.⁶ Based on the early work on conjugated polymers, it was thought that long exciton diffusion lengths were the main reason for the large changes in film luminescence in the presence of the explosive. That is, there was efficient PET in the film. However, there have been fewer studies exploring the role of analyte diffusion within the films and ascertaining its relative importance in determining the performance of film-based sensors. We have previously shown through quartz crystal microbalance measurements of the vapour uptake in films of conjugated sensing materials that the vapour diffusion process dominates the sensing performance of both polymeric and non-polymeric sensing materials in real-time sensing.¹¹ As a consequence, polymeric and non-polymeric sensing materials can exhibit comparable sensing performance despite their different material characteristics. More recently, poly(dendrimer)s have emerged as a new class of luminescent material. Although they were originally designed as the light-emitting material for organic light-emitting diodes,¹² it has been shown that fluorescent poly(dendrimer)s can also be used as sensing materials for nitro group-containing explosives.^{13,14} Fluorescent poly(dendrimers) are generally composed of a flexible non-conjugated polymer backbone with bulky fluorescent dendritic side chains. Initial studies on the use of poly(dendrimer)s for the detection of explosives have shown promising results in both solution-based and thin film-based studies. However, it still remains unclear how varying the dendritic side chains and surface groups may affect the performance in the solid state and therefore how to optimise the design of such materials.

In this study, we investigate poly(dendrimer)s as solid-state sensing materials for the detection of nitroaliphatic and nitroaromatic vapours (Fig. 1). The poly(dendrimer)s **P1** and **P2** are composed of norbornenyl-derived polymer backbones and triphenylamine-based dendritic side chains with 9,9-di-*n*-propylfluorenyl moieties attached to two of the phenyl groups. In addition, **P2** has a larger branched structure through the addition of first-generation 'G1' biphenyl dendrons with 2-ethylhexyloxy groups attached. The dendritic side chains provide differences in the steric bulk, which can affect the solid-state properties. The synthesis and characterisation of **P1** and **P2** as well as their sensing performance in solution-based measurements have been previously reported.¹⁴ However, it is important to note that solution measurements are often not reflective of the film performance.¹⁵ The choice of the triphenylamine-based

chromophores for the poly(dendrimer)s is based on our previous observation that triphenylamine-based dendrimers exhibit selective responses to nitro-containing explosives.¹⁰ For this reason, we have included the related dendrimer **D1** as a comparison (Fig. 1). To evaluate the possible impact of the polymeric structure on the sensing properties, we employed nitro-containing analytes relevant to the detection of nitro-based explosives, which have been and continue to be used for industry and military applications. The two analytes were the nitroaliphatic taggant 2,3-dimethyl-2,3-dinitrobutane (DMNB), which is added to most commercially available plastic explosives, and the nitroaromatic 2,4-dinitrotoluene (2,4-DNT). 2,4-DNT can be found in impure 2,4,6-trinitrotoluene (TNT).

Results and discussion

Photophysical properties

The absorption and photoluminescence (PL) emission spectra for **P1**, **P2** and **D1** in the solid state are shown in Fig. 2. The absorbance spectra of **P1** and **P2** are similar at longer wavelengths, consistent with the similarities of the chromophores, which only differ by the single phenyl ring that forms the branching point of G1. At wavelengths below 350 nm, the absorbance differs owing to the presence of the first-generation biphenyl dendrons on **P2**, which absorb strongly at shorter wavelengths. Indeed, **D1**, which contains the same dendrons, also absorbs strongly at the shorter wavelengths. There is a small blue shift of the absorbance of **P1** and **P2** relative to **D1**, which reflects the larger chromophore of **D1**. That is, in the case of **D1**, the chromophore is delocalised over all three arms through the central nitrogen atom.¹⁶ The PL emission spectra of **P1** and **P2** are broadly similar, with **P2** exhibiting a small red shift relative to **P1**, which can be attributed to the presence of the dendrons and the resulting increase in the conjugation length (the branching phenyl group of G1 is part of the chromophore in **P2**). In contrast to the trend observed in the absorbance data, the peak of the PL emission of **D1** is slightly blue-shifted relative to that of the polymers with a narrower full-width at half maximum (FWHM). The photoluminescence quantum yield (PLQY) values in the solid state were determined to be $20.2 \pm 3.9\%$ for **P1** and $8.3 \pm 1.3\%$ for **P2**. Both values are significantly lower than the $\sim 60\%$ solution PLQY previously reported,¹⁴ suggesting that there are interpolymer interchromophore interactions and that these are not suppressed by the presence of the first-generation dendrons in **P2**. However, the fact that the PL emission for **P1** and **P2** is not significantly broader than that of **D1** suggests that the intermolecular interactions are not leading to the formation of aggregate or exciplex states. The film PLQY of **D1** is significantly higher than both polymers at $46.9 \pm 4.5\%$, although all are suitable for fluorescence-based detection.

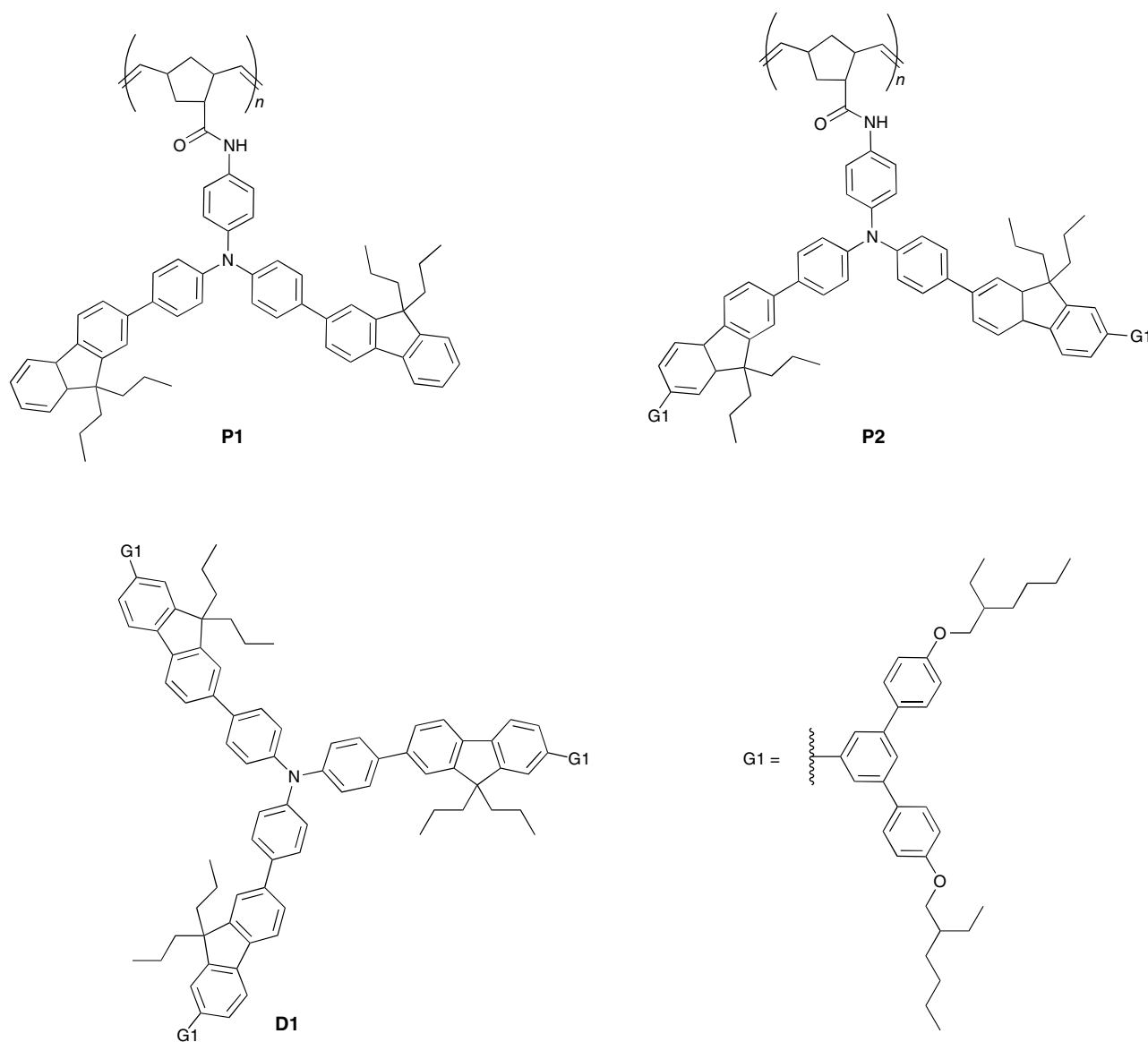


Fig. 1. Structures of the polymeric sensing materials **P1** and **P2**, the dendrimer **D1** and the first-generation biphenyl dendron **G1**. **P1** and **P2** had similar weight average molecular weights ($\bar{M}_{w,s}$) and dispersities (\bar{D}_s), being 2.4×10^4 and 3.5×10^4 , and 1.3 and 1.4 respectively.

Solid-state sensing performance

To evaluate the sensing performance of **P1** and **P2**, we measured the change in the PL emission intensity of thin films (~ 40 nm thick) exposed to a sequence of 'pulses' of 2,4-DNT or DMNB vapour of increasing concentration in a nitrogen stream. We note that solution Stern–Volmer measurements show that the poly(dendrimer)s have a greater affinity for 2,4-DNT relative to the corresponding monomer unit.¹⁴ In the case of DMNB, the vapour concentration was varied between ~ 0.1 and 1.6 ppm whereas for 2,4-DNT, the concentration range was ~ 3 –44 ppb. These concentrations are lower than the equilibrium vapour pressures of both analytes, which are 350 ppb for 2,4-DNT and 2.7 ppm for

DMNB.⁶ Shown in Fig. 3a are the film quenching responses of **P1** and **P2** to DMNB vapour with the vapour 'pulses' represented by the filled grey line. The fluorescence quenching responses of **P2** are greater in magnitude than those of **P1**, with the response to a concentration of ~ 0.1 ppm of DMNB evident in the data. By contrast, the lowest concentration at which there is a clear response of **P1** to DMNB is ~ 0.4 ppm, suggesting that the ~ 40 nm thick film of **P1** exhibits approximately four times lower sensitivity to DMNB than that of **P2**. The other way in which the responses of the polymers differ on exposure to DMNB is in the recovery of the fluorescence intensity after analyte exposure. **P2** shows significant recovery of the fluorescence intensity in the ~ 300 s between successive

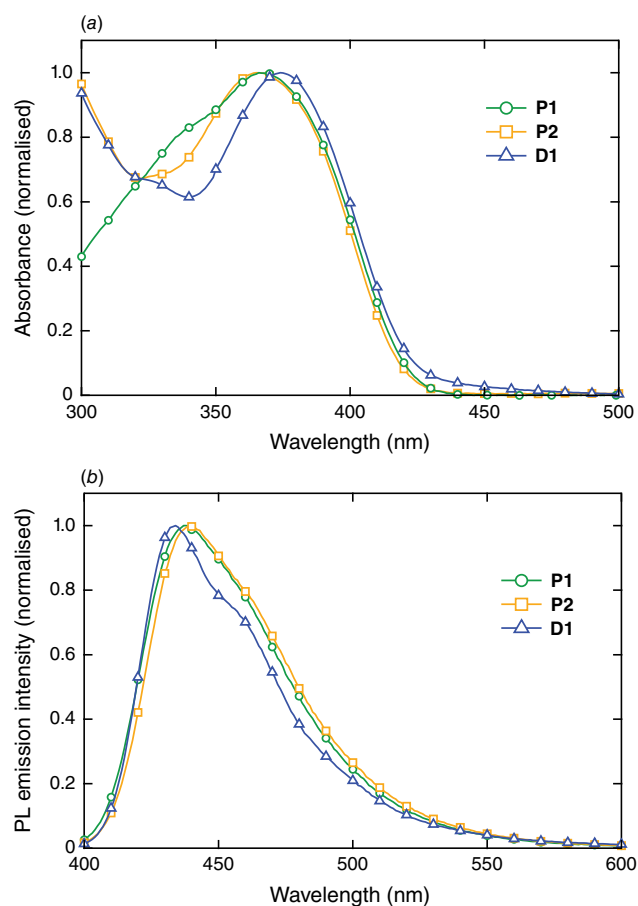


Fig. 2. (a) Absorption, and (b) PL emission of **P1**, **P2** and **D1**.

pulses of DMNB vapour when the sample was under a nitrogen flow. The greater fluorescence quenching and recovery of **P2** both suggest that the DMNB vapour moves more readily through the **P2** film than the **P1** film. DMNB is known to typically generate a weak PL response owing to its relatively low electron affinity and weaker intermolecular interactions compared with nitroaromatic analytes,^{17,18} so the results for **P2** are encouraging for potential deployment in a detector.

When films of **P1** and **P2** were exposed to 'pulses' of 2,4-DNT vapour, the behaviour of the two materials was more similar (see Fig. 3b), with responses detected for each exposure. The larger magnitude of the PL quenching responses is consistent with the higher electron affinity of 2,4-DNT when compared with DMNB, which leads to a more energetically favourable PET process, and the fact that it is aromatic means it can interact strongly with the side chain chromophores by π - π interactions. However, as was observed with exposure to DMNB vapour, the magnitude of the PL quenching response was greater for **P2** than **P1** with greater recovery of the fluorescence intensity after exposure. These observations suggest that the inclusion of the first-generation biphenyl dendrons in **P2** is beneficial for the penetration of both DMNB and 2,4-DNT into and diffusion out of the film, which is useful for a reusable sensor.

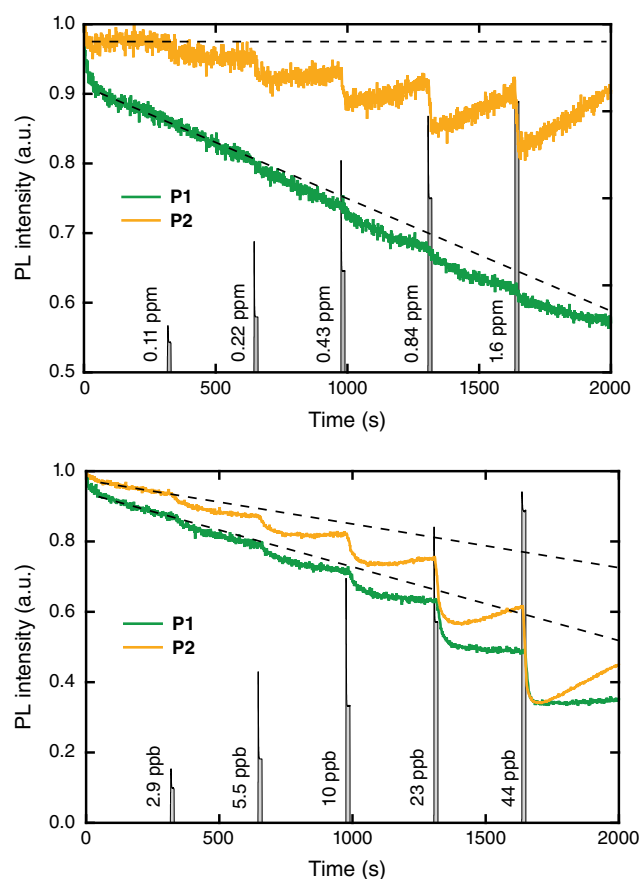


Fig. 3. Photoluminescence intensity of ~ 40 nm thick films of **P1** and **P2** to a sequence of exposures to vapour of (a) DMNB (note the 'dashed baselines' are to provide a guide to the eye for the smaller change in PL intensity), and (b) 2,4-DNT of increasing concentration. The films of **P1** were photoexcited at 352 nm with the PL intensity measured at 445 nm. The films of **P2** were photoexcited at 364 nm with the PL intensity measured at 449 nm. The analyte vapour 'pulses' are represented by the filled grey vertical lines and are annotated with the concentration. The decrease in the PL intensity in the absence of the analyte is due to photodegradation of the poly(dendrimer) films.

Neutron reflectometry

To better understand the PL quenching results for the films of **P1** and **P2** with DMNB and 2,4-DNT, we performed neutron reflectometry measurements using deuterated 2,4-DNT (*d*-DNT) to provide contrast with the non-deuterated sensing materials. We also included a film of **D1** in these experiments to compare the vapour absorption behaviour with a non-polymeric system with a similar chromophore. Previous studies have shown that the high sensitivity of amorphous films of conjugated sensing materials is due to the relatively high analyte concentration in the diffusion front that moves through the sensing film.¹¹ Neutron reflectometry measurements of films at equilibrium have been previously used to quantify the amount of analyte vapour absorbed and its distribution within the film.^{19,20}

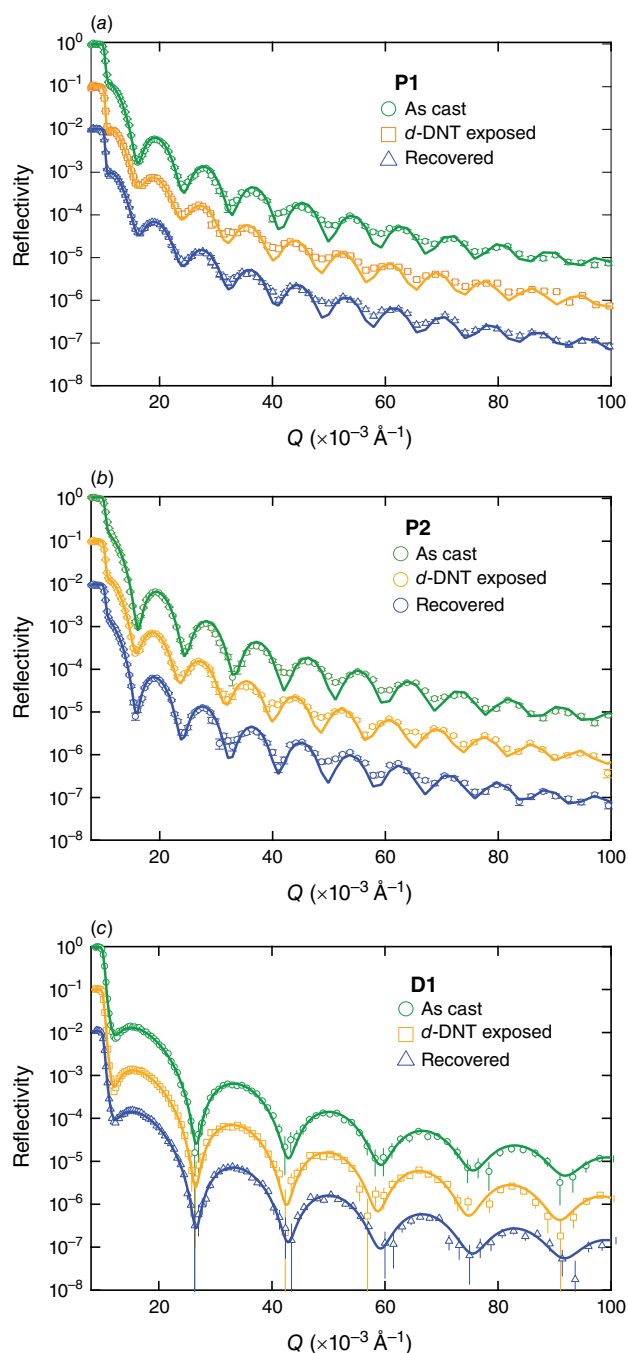


Fig. 4. Neutron reflectivity data and fits for spin-coated films of (a) **P1**, (b) **P2**, and (c) **D1** in their as-cast, saturated with *d*-DNT and recovered states.

The neutron reflectometry data for films of **P1**, **P2** and **D1** are shown in Fig. 4 in their as-cast state, when saturated with *d*-DNT vapour and after the recovery process, which consisted of exposing the films to a nitrogen flow (full details in the Experimental section). The reflectivity data include error bars and fits using a simple model consisting of two layers (SiO_2 and sensing material) and three interfaces (Si-SiO_2 , SiO_2 -sensing material and sensing material-air).

The scattering length density (SLD) profiles corresponding to the fits are shown in Fig. 5 alongside the PL data collected during the reflectometry measurements, which allowed us to correlate the analyte uptake with the PL quenching for each sensing material.

The data for the **P1** film (Fig. 5a, b) showed that the PL intensity was fully quenched when the film was saturated with *d*-DNT, with no significant increase of the emission intensity after the recovery process. This is consistent with the SLD profiles corresponding to the fits to the neutron reflectivity data, which show that the SLD of the film increased from 1.49×10^{-6} to $1.66 \times 10^{-6} \text{ \AA}^{-2}$ (see Table 1 for a summary of the neutron reflectivity data) and the thickness increased from 71.7 to 74.5 nm (see Table 2 for a summary of the film thickness values) or by 3.9%. These data are consistent with previous measurements on conjugated dendrimers for the detection of explosives that showed that the films swell to accommodate the uptake of the analyte, which is distributed throughout the film. After the recovery process, there was a slight reduction of the SLD value of the film to $1.61 \times 10^{-6} \text{ \AA}^{-2}$ and film thickness to 73.4 nm, which is consistent with a substantial amount of the analyte remaining within the film and the absence of a PL intensity increase. From the increase in the SLD of the film and the SLD of *d*-DNT, which we calculate to be $6.26 \times 10^{-6} \text{ \AA}^{-2}$, we can estimate the concentration of *d*-DNT within the film. For **P1**, we find that the concentration of *d*-DNT in the saturated film is $0.19 \text{ molecules nm}^{-3}$, which decreases to 0.14 nm^{-3} on placing under a nitrogen flow. This corresponds to an average separation between the *d*-DNT molecules of just 3.5 and 3.8 nm in the saturated and recovered **P1** films respectively, which is within the expected exciton diffusion length for an organic semiconductor and consistent with efficient PL quenching.²¹

The data for the **P2** film (Fig. 5c, d) show the same general behaviour as **P1** with a few notable differences. The SLD of the as-cast film is lower at $1.06 \times 10^{-6} \text{ \AA}^{-2}$ and the change in the SLD of the saturated film is significantly larger at $1.52 \times 10^{-6} \text{ \AA}^{-2}$. Also, the film thickness increases from 68.7 to 74.4 nm, which is an 8.3% change. These features are all consistent with the **P2** film absorbing a higher concentration of *d*-DNT, which we calculate to be $0.42 \text{ molecules nm}^{-3}$, approximately twice the *d*-DNT uptake capacity of **P1**. The SLD of the **P2** film decreases to $1.37 \times 10^{-6} \text{ \AA}^{-2}$ during the recovery process, which suggests that although $\sim 1/3$ of the *d*-DNT has been released from the film, there is still a significant concentration left within the film after the recovery ($0.28 \text{ molecules nm}^{-3}$). This is supported by the PL data, which shows no significant increase in the emission intensity of the **P2** film after the recovery process. To understand the reason for the greater uptake of the **P2** film, we compared the mass densities of the **P1** and **P2** films. These were calculated from the measured SLD values for the as-cast films and determined to be $1.01 \pm 0.01 \text{ g cm}^{-3}$ for **P1** and $0.91 \pm 0.01 \text{ g cm}^{-3}$ for **P2**.

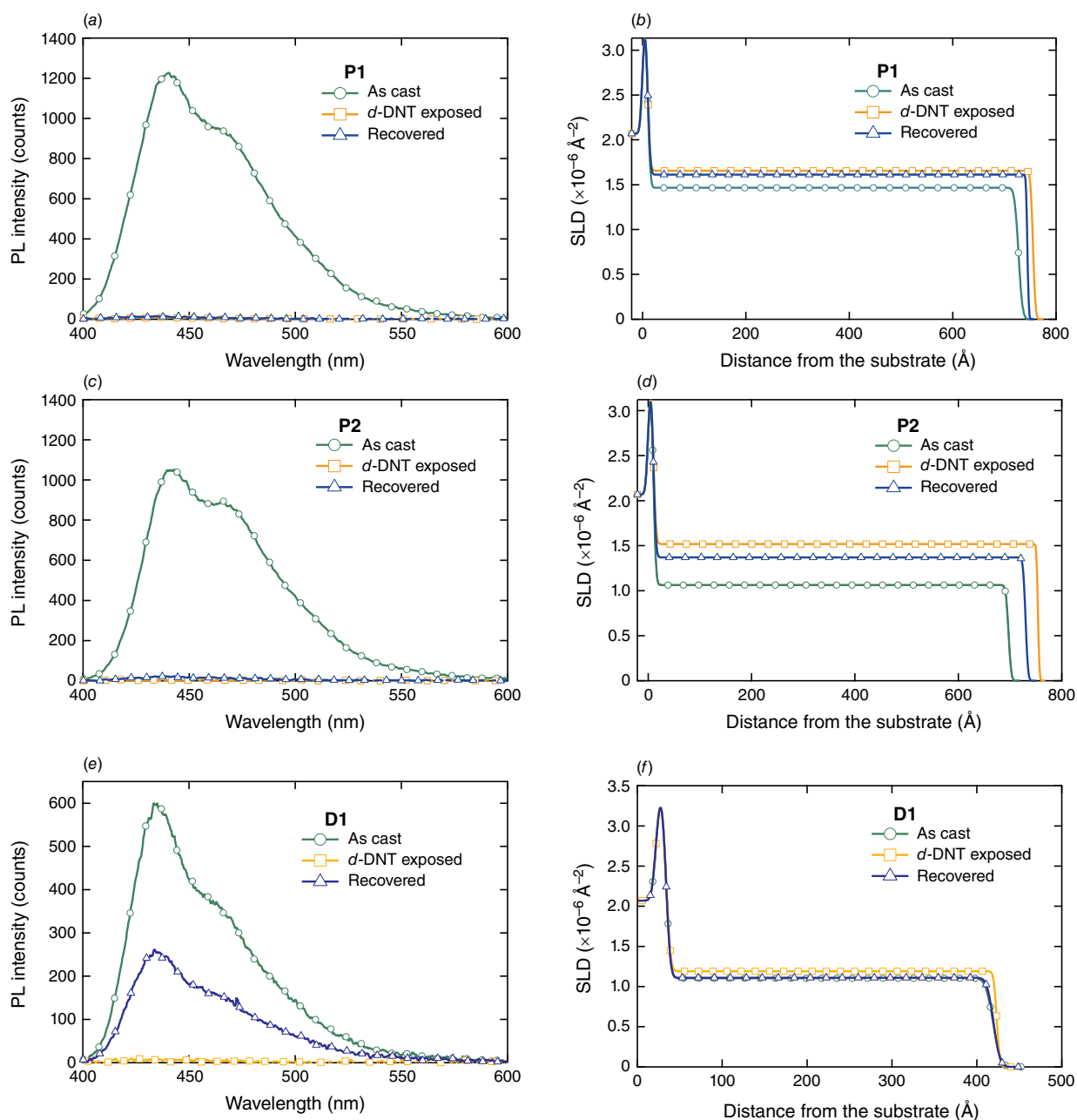


Fig. 5. PL intensity of films of (a) **P1**, (c) **P2**, and (e) **D1** – as cast, after exposure to *d*-DNT, and the subsequent removal of the analyte (recovery). (b, d, f) Corresponding changes in the SLD v. distance from substrate (thickness) for each of the materials.

Table 1. Summary of the film SLD data for **P1**, **P2** and **D1**.

	As-cast SLD ($\times 10^{-6} \text{ \AA}^{-2}$)	DNT-exposed SLD ($\times 10^{-6} \text{ \AA}^{-2}$)	Recovered SLD ($\times 10^{-6} \text{ \AA}^{-2}$)	DNT-exposed number density (<i>d</i> -DNT molecules nm^{-3})	Recovered number density (<i>d</i> -DNT molecules nm^{-3})
P1	1.47 ± 0.01	1.66 ± 0.01	1.61 ± 0.01	0.19	0.14
P2	1.06 ± 0.01	1.52 ± 0.01	1.37 ± 0.01	0.42	0.28
D1	1.10 ± 0.01	1.19 ± 0.01	1.11 ± 0.01	0.12	0.01

Table 2. Summary of film thickness data for **P1**, **P2** and **D1**.

	As-cast thickness (nm)	DNT-exposed (nm)	Recovered (nm)	Degree of swelling at saturation (%)
P1	71.7 ± 0.1	74.5 ± 0.1	73.4 ± 0.1	3.9 ± 0.2
P2	68.7 ± 0.1	74.4 ± 0.1	72.0 ± 0.1	8.3 ± 0.2
D1	38.5 ± 0.1	38.9 ± 0.1	38.6 ± 0.1	1.0 ± 0.4

Although the mass density for **P1** is typical for a dense organic semiconductor film, the lower mass density of **P2** suggests that the addition of the bulky dendrons reduces close packing of the polymer chains and potentially introduces micro-voids. The presence of such micro-voids is consistent with the increased uptake of the *d*-DNT and the observation of greater recovery in the PL quenching kinetics with DMNB and 2,4-DNT (see Fig. 3).

Finally, we compare the results for **P1** and **P2** with those for **D1** (Fig. 5e, f). The **D1** film also shows complete quenching of the PL intensity when saturated with *d*-DNT, with the SLD and thickness of the film increasing in a way that is consistent with the uptake of vapour within the film. However, the magnitude of the change was lower than that observed for **P1** and **P2**, with a *d*-DNT concentration in the saturated film of 0.12 molecules nm⁻³ and a negligible change in the thickness of the film (Table 2). Unlike the films of **P1** and **P2** though, the **D1** film regained approximately 50% of its PL intensity following the recovery process, which is consistent with the SLD of the recovered film returning to the same value measured for the as-cast state within experimental uncertainty. Interestingly, the mass density of the **D1** film was calculated to be 1.01 ± 0.01 g cm⁻³, which is in agreement with the previously reported value¹⁰ and the same as for **P1**. Hence, despite **P2** and **D1** featuring the same dendron structure, only the polymeric molecule showed a reduction in mass density consistent with increased steric bulk. That is, covalently linking the dendritic chromophores led to less efficient packing of the chromophores in the solid state.

Conclusions

We have studied two triphenylamine-based poly(dendrimer) materials with fluorenyl groups attached to two of the phenyl groups of the triphenylamine for the detection of nitro-based explosives and taggants and characterised their vapour-sensing properties in the solid state. We found that poly(dendrimer) **P2** with biphenyl dendrons attached to the fluorenyl groups exhibited greater sensitivity to vapours of DMNB and 2,4-DNT and photoluminescence recovery in pulsed sub-saturation analyte measurements than poly(dendrimer) **P1**, which did not have the biphenyl dendrons. Using neutron reflectometry, we quantified the vapour uptake of films of both poly(dendrimer)s to deuterated

2,4-DNT (*d*-DNT) and compared their behaviour with a triphenylamine-core dendrimer **D1** with a fluorenyl group on each arm and biphenyl dendrons. We found that **P1**, **P2** and **D1** exhibit similar *d*-DNT uptake behaviour, with each material absorbing the vapour, leading to the film thickness increasing. However, we found that **P2** exhibits approximately twice as much *d*-DNT uptake as **P1** and more than three times as much as **D1** at equilibrium. We correlate the greater capacity for analyte absorption with the lower mass density of **P2** compared with **P1** and **D1**, which we attribute to the increased steric bulk from the biphenyl branching groups and resulting micro-void formation. However, neither poly(dendrimer) exhibits as much photoluminescence recovery during the analyte saturation neutron reflectometry experiments as **D1**, suggesting that vapour diffusion is generally more inhibited in the poly(dendrimers). These results show how varying the branching groups within the poly(dendrimer) structure provides an additional molecular engineering approach with which to modulate vapour uptake and sensing performance in the solid state.

Experimental

Film preparation

Thin films for the photophysical measurements were prepared by spin-coating 5 or 15 mg mL⁻¹ solutions in double-distilled toluene onto fused silica substrates, using a Cookson Electronics SCS G3-8 spin-coater where the spin speed was 1000 or 2000 rpm. The film thicknesses on the fused silica substrates (12-mm diameter) were determined using a Bruker Dektak XT surface profiler and averaged over a minimum of five measurements across the film. Films for the neutron reflectometry measurements were spin-coated from chloroform solutions onto clean 2-inch (~5-cm) diameter silicon wafers, with the thicknesses determined from the measurements. The choice of film thickness was dependent on the ease of film formation (small *v.* large substrate) noting that the kinetics of analyte uptake have been previously reported to be independent of film thickness.¹¹

Photophysical characterisation

The thin film absorption and PL spectra were measured on a Varian Cary 5000 UV-Vis-NIR (NIR, near-infrared) spectrophotometer and a Horiba Jobin-Yvon Fluorolog-3

instrument respectively. Film PLQY measurements were performed following the method described by Greenham et al.²² The 325-nm output of a He–Cd laser was attenuated with neutral density filters and used to photoexcite the films. The PL signal was measured with a calibrated photodiode. The PLQY was measured at multiple points on each film and averaged over multiple films.

Vapour sensing characterisation

The investigation of the pulsed PL quenching properties of the sensing films was performed using a Horiba Jobin-Yvon Fluorolog 3 spectrometer fitted with a bespoke optical chamber connected to the output from two Bronkhorst mass flow controllers (MFCs). Analyte vapour was generated from a coiled segment of stainless steel tubing coated on the inside with the analyte. The analyte coil was placed downstream from one of the MFCs and then the output was mixed by a valve with the nitrogen flow (1 L min^{-1}) from the second MFC. The system was controlled by a LabView-based interface that recorded the dilution values of the analyte flow. The analyte coil was calibrated by passing known volumes of the analyte flow through a series of three bubblers containing acetonitrile and then measuring the absorbance of these solutions to determine the concentration of the captured analyte. The analyte absorbance in the solution from the final bubbler in the series was negligible, confirming that the system was capturing all the analyte vapour. Films were excited at the peak absorption wavelength and the change in PL intensity was monitored at the wavelength corresponding to the emission peak.

Neutron reflectometry

Neutron reflectometry was performed with the Platypus time-of-flight neutron reflectometer (Australian Centre for Neutron Scattering, ANSTO, Sydney, Australia) using a cold neutron spectrum ($2.8 \text{ \AA} < \lambda < 18.0 \text{ \AA}$).²³ The beam was mechanically chopped (EADS Astrium GmbH) at 20 Hz to generate neutron pulses in medium resolution mode ($\Delta\lambda/\lambda = 4\%$). The scattered neutrons were recorded on a two-dimensional helium-3 neutron detector (Denex GmbH). Reflected beam spectra were collected at 0.65 and 2.5° for 1 and 2 h respectively. The reflectivity profiles were analysed using the Motofit reflectometry analysis program.²⁴ All of the neutron reflectometry fits were modelled with a $5\text{--}6 \text{ \AA}$ thick oxide layer on the surface of the silicon substrates with an SLD of $3.47 \times 10^{-6} \text{ \AA}^{-2}$. The SLD of silicon was taken to be $2.07 \times 10^{-6} \text{ \AA}^{-2}$. The films were exposed to a saturated atmosphere of the analytes for 5 h, which was significantly longer than the time reported for **D1** and other conjugated polymers to reach equilibrium (usually 1–2 h).^{10,11} The cell in which the measurements were made also contained an analyte vapour source to maintain the film saturation.

References

- Salinas Y, Martínez-Máñez R, Marcos MD, Sancenón F, Costero AM, Parra M, Gil S. Optical chemosensors and reagents to detect explosives. *Chem Soc Rev* 2012; 41: 1261–1296. doi:10.1039/C1CS15173H
- Sun X, Wang Y, Lei Y. Fluorescence based explosive detection: from mechanisms to sensory materials. *Chem Soc Rev* 2015; 44: 8019–8061. doi:10.1039/C5CS00496A
- Caron T, Guillemot M, Montméat P, Veignal F, Perraut F, Prené P, Serein-Spirau F. Ultra trace detection of explosives in air: development of a portable fluorescent detector. *Talanta* 2010; 81: 543–548. doi:10.1016/j.talanta.2009.12.040
- Moore DS. Instrumentation for trace detection of high explosives. *Rev Sci Instruments* 2004; 75: 2499–2512. doi:10.1063/1.1771493
- Yang JS, Swager TM. Fluorescent porous polymer films as TNT chemosensors: electronic and structural effects. *J Am Chem Soc* 1998; 120: 11864–11873. doi:10.1021/ja982293q
- Shaw PE, Burn PL. Real-time fluorescence quenching-based detection of nitro-containing explosive vapours: what are the key processes? *Phys Chem Chem Phys* 2017; 19: 29714–29730. doi:10.1039/C7CP04602B
- Thomas SW, Joly GD, Swager TM. Chemical sensors based on amplifying fluorescent conjugated polymers. *Chem Rev* 2007; 107: 1339–1386. doi:10.1021/cr0501339
- Zhou Q, Swager TM. Fluorescent chemosensors based on energy migration in conjugated polymers: the molecular wire approach to increased sensitivity. *J Am Chem Soc* 1995; 117: 12593–12602. doi:10.1021/ja00155a023
- Shaw PE, Cavaye H, Chen SSY, James M, Gentle IR, Burn PL. The binding and fluorescence quenching efficiency of nitroaromatic (explosive) vapors in fluorescent carbazole dendrimer thin films. *Phys Chem Chem Phys* 2013; 15: 9845–9853. doi:10.1039/c3cp51372f
- Geng Y, Ali MA, Clulow AJ, Fan S, Burn PL, Gentle IR, Meredith P, Shaw PE. Unambiguous detection of nitrated explosive vapours by fluorescence quenching of dendrimer films. *Nat Commun* 2015; 6: 8240. doi:10.1038/ncomms9240
- Ali MA, Geng Y, Cavaye H, Burn PL, Gentle IR, Meredith P, Shaw PE. Molecular versus exciton diffusion in fluorescence-based explosive vapour sensors. *Chem Commun* 2015; 51: 17406–17409. doi:10.1039/C5CC06367A
- Russell SM, Jang J, Brewer AM, Stoltzfus DM, Puttock EV, Burn PL. A red emissive poly(dendrimer) for solution processed organic light-emitting diodes. *Organic Electronics* 2020; 78: 105594. doi:10.1016/j.orgel.2019.105594
- Loch AS, Stoltzfus DM, Burn PL, Shaw PE. High-sensitivity poly(dendrimer)-based sensors for the detection of explosives and taggant vapors. *Macromolecules* 2020; 53: 1652–1664. doi:10.1021/acs.macromol.0c00060
- Hutchinson KL, Stoltzfus DM, Burn PL, Shaw PE. Luminescent poly(dendrimer)s for the detection of explosives. *Mater Adv* 2020; 1: 837–844. doi:10.1039/D0MA00249F
- Cavaye H, Shaw PE, Wang X, Burn PL, Lo SC, Meredith P. Effect of dimensionality in dendrimeric and polymeric fluorescent materials for detecting explosives. *Macromolecules* 2010; 43: 10253–10261. doi:10.1021/ma102369q
- Lupton JM, Samuel IDW, Burn PL, Mukamel S. Control of intrachromophore excitonic coherence in electroluminescent conjugated dendrimers. *J Phys Chem B* 2002; 106: 7647–7653. doi:10.1021/jp020418e
- Thomas III SW, Amara JP, Bjork RE, Swager TM. Amplifying fluorescent polymer sensors for the explosives taggant 2,3-dimethyl-2,3-dinitrobutane (DMNB). *Chem Commun* 2005; 36: 4572–4574. doi:10.1039/b508408c
- Clulow AJ, Burn PL, Meredith P, Shaw PE. Fluorescent carbazole dendrimers for the detection of nitroaliphatic taggants and accelerants. *J Mater Chem* 2012; 22: 12507–12516. doi:10.1039/c2jm32072j
- Cavaye H, Smith ARG, James M, Nelson A, Burn PL, Gentle IR, Lo SC, Meredith P. Solid-state dendrimer sensors: probing the diffusion of an explosive analogue using neutron reflectometry. *Langmuir* 2009; 25: 12800–12805. doi:10.1021/la9017689

- 20 Cavaye H, Shaw PE, Smith ARG, Burn PL, Gentle IR, James M, Lo SC, Meredith P. Solid state dendrimer sensors: effect of dendrimer dimensionality on detection and sequestration of 2,4-dinitrotoluene. *J Phys Chem C* 2011; 115: 18366–18371. doi:10.1021/jp205586s
- 21 Mikhnenko OV, Blom PWM, Nguyen TQ. Exciton diffusion in organic semiconductors. *Energy Environ Sci* 2015; 8: 1867–1888. doi:10.1039/C5EE00925A
- 22 Greenham NC, Samuel IDW, Hayes GR, Phillips RT, Kessener YARR, Moratti SC, Holmes AB, Friend RH. Measurement of absolute photoluminescence quantum efficiencies in conjugated polymers. *Chem Phys Lett* 1995; 241: 89–96. doi:10.1016/0009-2614(95)00584-Q
- 23 James M, Nelson A, Holt SA, Saerbeck T, Hamilton WA, Klose F. The multipurpose time-of-flight neutron reflectometer 'Platypus' at Australia's OPAL reactor. *Nucl Instrum Meth Phys Res Sect A* 2011; 632: 112–123. doi:10.1016/j.nima.2010.12.075
- 24 Nelson A. Co-refinement of multiple-contrast neutron/X-ray reflectivity data using MOTOFIT. *J Appl Crystallogr* 2006; 39: 273–276. doi:10.1107/S0021889806005073

Data availability. Data are available on reasonable request from the authors.

Conflicts of interest. The authors declare that they have no conflicts of interest.

Declaration of funding. This research did not receive any specific funding.

Acknowledgements. P. L. Burn was awarded the RACI Applied Research Medal 2022. The authors thank Andrew Nelson, Jake McEwan and Benjamin Robeck for their assistance with the neutron reflectometry. The authors acknowledge the Australian Centre for Neutron Scattering of the Australian Nuclear Science and Technology Organisation (ANSTO), the Australian Institute for Nuclear Science and Engineering (AINSE) for providing the neutron research facilities for the reflectometry experiments, and the Australian National Deuteration Facility for providing the deuterated *d*-DNT. The NDF is partly supported by the National Collaborative Research Infrastructure Strategy, an initiative of the Australian Government.

Author affiliation

^ACentre for Organic Photonics & Electronics, School of Chemistry and Molecular Biosciences, The University of Queensland, Qld 4072, Australia.